V International Conference on Computational Methods for Coupled Problems in Science and Engineering
COUPLED PROBLEMS 2013
S. Idelsohn, M. Papadrakakis and B. Schrefler (Eds)

ANISOTROPIC DIFFUSION AND PROPAGATION OF SOUND WAVES IN POROELASTIC MEDIA

BETTINA ALBERS[*] AND KRZYSZTOF WILMANSKI[†]

[*] Department for Soil Mechanics and Geotechnical Engineering
Technische Universität Berlin (TU Berlin)
Sekr. TIB1-B7, Gustav-Meyer-Allee 25, 13355 Berlin, Germany
e-mail: albers@grundbau.tu-berlin.de, www.mech-albers.de

[†] TU Berlin, Germany and ROSE School Pavia, Italy
http://en.wikipedia.org/wiki/Krzysztof_Wilmanski

Key words: Anisotropy of tortuosity, Acoustic Waves, Poroelastic Media, Shear Polarization.

Abstract. In an earlier paper it was already suggested that the anisotropy of the tortuosity yields essential changes of the attenuation of the waves in poroelastic media depending on the propagation direction in relation to the principal directions of tortuosity and on the mode of the wave. In the region of low frequencies appearing in geotechnical applications the orientation of the principal directions of tortuosity plays a secondary role in measured speeds and attenuations and most likely cannot be used for practical purposes. However, due to the appearance of two shear waves anyway the construction of a device for measuring the anisotropy of the permeability may be possible. It would have to induce shear waves of different polarization and different propagation directions. Then, also for the range of low frequencies, one could measure the principal values and directions of the tortuosity by comparing the amplitudes of arrivals for different polarization of the signals.

1 INTRODUCTION

In elastic solids the anisotropy of a material (e.g. of wood or fibre-reinforced synthetics) enters a model through the constitutive law. The relation between stresses and deformations is described by a generalized Hooke law in which the elasticity tensor is of fourth order. The number of elastic constants (the coefficients of the elasticity tensor) can be reduced from 81 by considering special cases of anisotropy (e.g. for monoclinic symmetry to 13, for orthotropic symmetry to 9 or for transversal isotropy to 5). For isotropic solid materials only two independent elastic constants, e.g. the Lamé parameters λ and μ, remain.

In poroelastic materials the relative motion of fluid components with respect to the skeleton, i.e. the diffusion, is of high importance. This characteristic feature of a permeable porous material distinguishes porous materials from other multicomponent systems such as composites. The macroscopic permeability of a porous medium is influenced by the microstructure of the solid material, in particular, by the shape of the channels and their volume contribution to the total volume of the material. The permeability characterizes the intensity of diffusion. In the description of rocks and porous materials deformations of the

anisotropic skeleton are less important than anisotropic diffusion properties. Therefore, here, the anisotropy of the material is described not by anisotropic stress-strain relations but by anisotropic permeability. It is induced by a symmetric tensor of permeability defined by a permeability coefficient and an inverse of the tortuosity tensor introduced by Bear and Bachmat [4].

Four modes of propagation arise by use of this model. For the special choice of orientation of the propagation direction these are two pseudo longitudinal modes *P*1 and *P*2, one pseudo transversal mode *S*2 and one transversal mode *S*1. Speeds of propagation and the attenuation of these waves as well as the polarization properties in dependence on the orientation of the principal directions of the tortuosity are presented.

2 GOVERNING EQUATIONS INCLUDING ANISOTROPIC PERMEABILITY

The two-component model of a poroelastic material including anisotropic permeability has been already presented in [1] and [6]. Its linearized partial momentum balances have the form

$$\rho^S \frac{\partial \mathbf{v}^S}{\partial t} = \operatorname{div} \mathbf{T}^S + \hat{\mathbf{p}}, \quad \rho^F \frac{\partial \mathbf{v}^F}{\partial t} = -\operatorname{grad} p^F - \hat{\mathbf{p}}, \tag{1}$$

where ρ^S and ρ^F are the initial constant partial mass densities of solid and fluid, $\mathbf{v}^S$ and $\mathbf{v}^F$ are the partial velocities of these two components. The partial stress tensor $\mathbf{T}^S$, the partial pressure p^F and the momentum source $\hat{\mathbf{p}}$ are given by the constitutive relations

$$\mathbf{T}^S = \mathbf{T}_0^S + \lambda^S e\mathbf{1} + 2\mu^S \mathbf{e}^S + Q\varepsilon\mathbf{1}, \; p^F = p_0^F - Qe - \rho^F \kappa \varepsilon, \; \hat{\mathbf{p}} = \pi_{ij}\left(\mathbf{v}_j^F - \mathbf{v}_j^S\right)\mathbf{e}_i, \tag{2}$$

where λ^S, μ^S, κ and Q are material parameters describing an isotropic poroelastic skeleton, an ideal fluid (with compressibility κ) and the coupling of both. Quantities with index zero are initial values and $\mathbf{e}_i$ are Cartesian base vectors, i.e. $\mathbf{e}_i \cdot \mathbf{e}_j = \delta_{ij}$. With $\mathbf{e}^S$ denoting the Almansi-Hamel tensor for small deformations of the solid, the volume changes of skeleton and fluid are $e = \operatorname{tr} \mathbf{e}^S$ and ε, respectively. The following compatibility conditions are satisfied

$$\frac{\partial \mathbf{e}^S}{\partial t} = \operatorname{sym} \operatorname{grad} \mathbf{v}^S, \quad \frac{\partial \varepsilon}{\partial t} = \operatorname{div} \mathbf{v}^F. \tag{3}$$

The matrix π_{ij} describes Cartesian components of the symmetric and positive definite permeability tensor. The influence of inertial forces attributed to added mass effects (i.e. the influence of relative accelerations) is neglected in this model. As pointed out in [7], in our opinion, it is erroneous to relate these forces to tortuosity effects as is often done in the literature. Moreover, such effects seem to be of higher order of magnitude.

The permeability tensor π_{ij} is the product of a positive scalar which reflects the physical conditions of diffusion $\pi_0 = \frac{\mu_v b}{D_h^2} \frac{g\rho_0^F}{n_0}$ and of the inverse of the tortuosity matrix T_{ij}^{-1} which is reflecting geometrical properties of the curvy channels. The former depends on the hydraulic diameter D_h, the initial porosity n_0, the true dynamic viscosity of the fluid in the pores μ_v, the capillary shape factor b and the earth gravity g. The latter has been introduced and discussed by Bear and Bachmat in [4]. If the direction $\mathbf{e}_3$ is chosen as the principal direction $\mathbf{t}_3$ of the symmetric tortuosity tensor the latter can be written in the following spectral form

$$\mathbf{T} = T_{ij}\mathbf{e}_i \otimes \mathbf{e}_j = \sum_{\mu=1}^{3} \frac{1}{\tau^{(\mu)2}} \mathbf{t}_\mu \otimes \mathbf{t}_\mu, \qquad \text{with } \mathbf{e}_3 = \mathbf{t}_3, \mathbf{e}_2 \cdot \mathbf{t}_1 = \sin\alpha, \mathbf{e}_1 \cdot \mathbf{t}_1 = \mathbf{e}_2 \cdot \mathbf{t}_2 = \cos\alpha \text{ and } \mathbf{e}_1 \cdot \mathbf{t}_2 = -\sin\alpha. \tag{4}$$

The tortuosity tensor possesses three real eigenvalues $\left\{\frac{1}{\tau^{(1)}}, \frac{1}{\tau^{(2)}}, \frac{1}{\tau^{(3)}}\right\}$ and three corresponding eigenvectors $\{\mathbf{t}_1, \mathbf{t}_2, \mathbf{t}_3\}$. The so-called principle tortuosities $\left\{\tau^{(1)}, \tau^{(2)}, \tau^{(3)}\right\}$, according to Bear and Bachmat [4], measure an average inverse of the cosines of the angles between a short straight interval in a chosen principal direction and a streamline between the endpoints of this interval.

3 MONOCHROMATIC WAVES

In this paper, the Cartesian reference system is chosen in which the relations $\mathbf{e}_3 = \mathbf{t}_3$, $\mathbf{e}_2 \cdot \mathbf{t}_1 = \sin\alpha$, $\mathbf{e}_1 \cdot \mathbf{t}_1 = \mathbf{e}_2 \cdot \mathbf{t}_2 = \cos\alpha$ and $\mathbf{e}_1 \cdot \mathbf{t}_2 = -\sin\alpha$ between the base vectors and the principal directions of the tortuosity are satisfied. The propagation of monochromatic waves of a given frequency ω in a two-component poroelastic material is investigated by use of the above presented model. The waves are solutions of the governing equations and result from the following presumptions

$$\begin{aligned} &\mathbf{v}^S = \mathbf{V}^S \mathrm{E}, \quad \mathbf{v}^F = \mathbf{V}^F \mathrm{E}, \quad \mathbf{e}^S = \mathbf{E}^S \mathrm{E}, \quad \varepsilon = E^F \mathrm{E}, \\ &\mathrm{E} = \mathrm{e}^{i(\mathbf{k}\cdot\mathbf{x}-\omega t)} \equiv \mathrm{e}^{-((\mathrm{Im}k)\mathbf{n}\cdot\mathbf{x})} \mathrm{e}^{i\mathrm{Re}k(\mathbf{n}\cdot\mathbf{x}-c_{ph}t)}, \\ &\mathbf{k} = k\mathbf{n}, \quad \mathbf{n} = \mathbf{e}_1, \quad \mathbf{n}\cdot\mathbf{n} = 1, \quad c_{ph} = \frac{\omega}{\mathrm{Re}\,k}, \end{aligned} \tag{5}$$

where $\mathbf{V}^S, \mathbf{V}^F, \mathbf{E}^S$ and $\mathbf{E}^F$ are constant amplitudes, $\mathbf{k}$ is the wave vector, k the wave number, $\mathbf{n}$ denotes the propagation direction and c_{ph} is the propagation speed of the monochromatic wave of frequency ω.

Applying (5) to Eq. (2) yields

$$\mathbf{E}^S = -\frac{1}{2\omega}\left(\mathbf{V}^S \otimes \mathbf{k} + \mathbf{k} \otimes \mathbf{V}^S\right), \quad E^F = -\frac{1}{\omega}\mathbf{V}^F \cdot \mathbf{k}. \tag{6}$$

From the momentum balances together with the constitutive relations the following eigenvalue problem arises

$$\begin{aligned} &\left(-\rho^S\omega^2\mathbf{1} + \lambda^S \mathbf{k}\otimes\mathbf{k} + \mu^S\left(k^2\mathbf{1} + \mathbf{k}\otimes\mathbf{k}\right) - i\pi_0\omega\mathbf{T}^{-1}\right)\mathbf{V}^S + \\ &\quad + \left(Q\mathbf{k}\otimes\mathbf{k} + i\pi_0\omega\mathbf{T}^{-1}\right)\mathbf{V}^F = 0, \\ &\left(Q\mathbf{k}\otimes\mathbf{k} + i\pi_0\omega\mathbf{T}^{-1}\right)\mathbf{V}^S + \left(-\rho^F\omega^2\mathbf{1} + \rho^F\kappa\mathbf{k}\otimes\mathbf{k} - i\pi_0\omega\mathbf{T}^{-1}\right)\mathbf{V}^F = 0. \end{aligned} \tag{7}$$

Since it is assumed that $\mathbf{n} = \mathbf{e}_1$, Eq. (7) can be simplified:

$$\begin{aligned} &-\rho^S\omega^2\mathbf{V}^S + \lambda^S k^2 \mathbf{e}_1 V_1^S + \mu^S\left(k^2\mathbf{V}^S + k^2\mathbf{e}_1 V_1^S\right) - i\pi_0\omega\mathbf{T}^{-1}\mathbf{V}^S + \\ &\quad + Qk^2\mathbf{e}_1 V_1^F + i\pi_0\omega\mathbf{T}^{-1}\mathbf{V}^F = 0, \qquad \mathbf{V}^S = V_i^S\mathbf{e}_i, \quad \mathbf{V}^F = V_i^F\mathbf{e}_i, \\ &Qk^2\mathbf{e}_1 V_1^S + i\pi_0\omega\mathbf{T}^{-1}\mathbf{V}^S - \rho^F\omega^2\mathbf{V}^F + \rho^F\kappa k^2\mathbf{e}_1 V_1^F - i\pi_0\omega\mathbf{T}^{-1}\mathbf{V}^F = 0. \end{aligned} \tag{8}$$

It is assumed that one of the principal directions of $\mathbf{T}$ is perpendicular to $\mathbf{k}$, i.e. $\mathbf{k} = k\mathbf{n} = k\mathbf{e}_1$ and $\mathbf{t}_3 = \mathbf{e}_3$. This simplifying assumption, which was also proposed in [1], causes that one of the propagation modes is purely transversal. In [6] the even simpler case was considered that the propagation direction $\mathbf{k}$ coincides with the direction $\mathbf{e}_1$ and simultaneously with one of the

principal directions of the tortuosity tensor, i.e. $\alpha = 0$.

3.1 Decoupled transversal wave

Multiplication of Eqs. (3) with $\mathbf{e}_3$ yields two equations for the two components V_3^S and V_3^F. Combination of these equations yields the dispersion relation

$$\left(\omega^2 - \frac{\mu^S}{\rho^S}k^2 + \frac{i\pi_0\omega}{\rho^S}\tau^{(3)2}\right)\left(\omega^2 + \frac{i\pi_0\omega}{\rho^F}\tau^{(3)2}\right) + \frac{\rho^F}{\rho^S}\left(\frac{\pi_0\omega}{\rho^F}\tau^{(3)2}\right) = 0, \tag{9}$$

where (4) has been used and $V_3^S \neq 0,\ \ V_3^F \neq 0$. Since the remaining components of the vectors $\mathbf{V}^S$ and $\mathbf{V}^F$ are zero, the result is clearly a transversal wave, i.e. its amplitude is perpendicular to the propagation direction. The existence of such a purely transversal *S*1-wave follows from the assumption that the eigenvector of the tortuosity tensor $\mathbf{t}_3$ is orthogonal to the propagation direction $\mathbf{n}$. Relation (9) yields the phase speeds and the attenuations of the *S*1-wave which are illustrated in Figure 1 for different values of the principal tortuosity $\tau^{(3)}$.

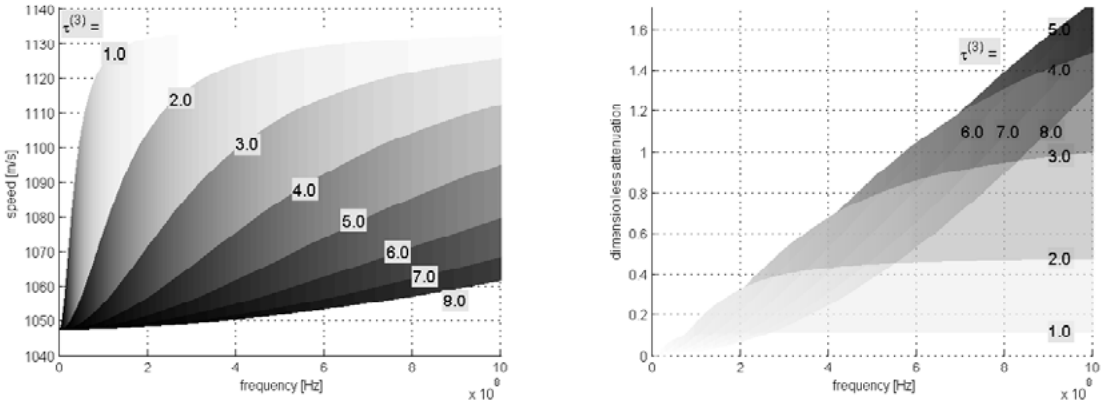

Figure 1: Speeds (left) and dimensionless attenuations (right) of the purely transversal wave appearing in Alermoehe sandstone for different values of the principal tortuosity $\tau^{(3)}$

For the illustration of the wave properties in this paper roughly data of Arnold [3] for Alermoehe sandstone saturated by water (Table 1) are used. She reported on tortuosities in the interval between 1.06 and 6.50. Similar results are obtained by Wang et al. [5] who measured values between 3.45 and 7.69 for the tortuosity of various rocks. Combining these results, here, $\tau^{(3)}$ is chosen between 1 and 8.

The value of the shear modulus $\mu^S = \frac{3}{2}K_d(1-2\nu)/(1+\nu)$ follows from Gassmann and Geertsma relations (for details see e.g. [2]).

3.2 Coupled waves

In order to achieve the phase speeds and attenuations of the coupled waves, Eqs. (3) have to be multiplied with $\mathbf{e}_1$ and $\mathbf{e}_2$. This yields four equations for the four unknown components V_1^S, V_2^S, V_1^F and V_2^F. Thus, the set of equations $\mathbf{AX} = \mathbf{0}$ has to be solved. The components of matrix $\mathbf{A}$ depend on the frequency, on the angle α reflecting the anisotropy of the tortuosity

Table 1: Example of the construction of one table

K_s	K_f	ν	n_0	ρ^{SR}	ρ^S	ρ^F
48 GPa	2.25 GPa	0.2	0.3	2500 $\frac{\text{kg}}{\text{m}^3}$	1750 $\frac{\text{kg}}{\text{m}^3}$	300 $\frac{\text{kg}}{\text{m}^3}$
λ^S	μ^S	κ	Q	K_d	K_w	π_0
1.5 GPa	2.25 GPa	$2.05\cdot10^6$ $\frac{\text{m}^2}{\text{s}^2}$	1.304 GPa	3 GPa	6.76 GPa	10^{10} $\frac{\text{kg}}{\text{m}^3\text{s}}$

K_s, K_f – true compressibility moduli of solid and fluid, ν – Poisson number, n_0 – initial porosity, $K_d = K_s/(1+50n_0)$, ρ^{SR}, ρ^S – true and partial mass densities of the solid, ρ^F – partial mass density of the fluid, λ^S, μ^S – Lamé parameters, κ – compressibility, Q – coupling parameter, $K_w = \left[(1-n_0)/K_s + n_0/K_f\right]^{-1}$, π_0 – permeability coefficient.

(introduced in (4)) and on the material parameters $\{\rho^S, \rho^F, \lambda^S, \mu^S, \kappa, Q, \pi_0, \tau^{(1)}, \tau^{(2)}, \tau^{(3)}\}$. A complete presentation of Matrix **A** can be found in [1]. Vector **X** is defined by $\mathbf{X} := \left(V_1^S, V_2^S, V_1^F, V_2^F\right)^T$. The dispersion relation det (**A**) = 0 determines the relation between ω and k. For a given real frequency ω three complex solutions for the wave number k are obtained. From these follow the phase speeds $\omega/(\text{Re } k)$ and the attenuations Im k. The solutions, illustrated in Figure 2, besides on frequency and the values of principle tortuosities, depend on the angle α. For values of the angle different from the limit values $\alpha = 0$ and $\alpha = \pi/2$ the modes of propagation are neither longitudinal nor transversal.

The phase speeds and dimensionless attenuations shown in Figures 1 and 2 are illustrated for a very large range of frequencies even if it is known that such high frequencies do not appear in geophysics. However, this is done in order to indicate the asymptotic properties of the waves. In view of a better comparability the attenuation is normalized by $\text{Im}\, k \to c_\infty \sqrt{2}/\omega_0 \,\text{Im}\, k$ where c_∞ is the high frequency limit of the phase speed. In Figures 2-4 three different choices of pairs of principal tortuosities are chosen, i.e. $\tau^{(1)} = 1.5$ and $\tau^{(2)} = 6$, $\tau^{(1)} = 2$ and $\tau^{(2)} = 4.5$ as well as $\tau^{(1)} = 2.8$ and $\tau^{(2)} = 3.2$.

The wave with the highest speed and the lowest attenuation is the fast longitudinal wave pseudo *P*1. The medium speed and attenuation belong to the pseudo *S*2 wave. The smallest

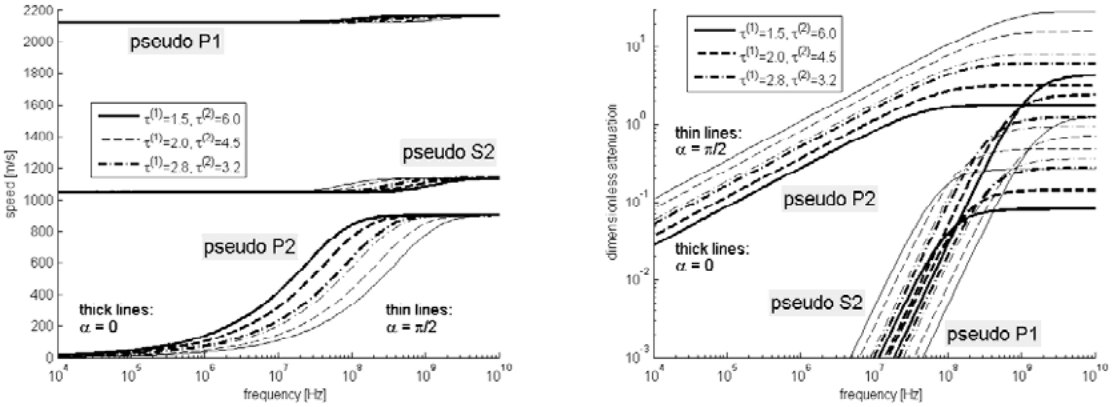

Figure 2: Speeds (left) and dimensionless attenuations (right) of the three pseudo waves appearing in Alermoehe sandstein for three pairs of principal tortuosities and two values of angle α

speed and the highest attenuation are those of the slow longitudinal wave pseudo *P*2. It is obvious that for both waves which exhibit high- and low-frequency limits different from zero, the pseudo *P*1 and the pseudo *S*2-wave, only at very high frequencies the angle α plays any role for the wave speed. The attenuations exhibit a strong dependence on the angle α predominantly for high values of the frequency. As for the classical *P*1- and *S*-waves of isotropic porous media the attenuation is rather small for the pseudo *P*1- and pseudo *S*2-wave. The maximum value for pseudo *P*1 is 1.25, for pseudo *S*2 it is around 4.5. The *P*2-wave in isotropic porous media is strongly damped. This is also the case for the pseudo *P*2-wave. The corresponding maximal dimensionless attenuation is 28. The values of the dimensionless attenuations indicate a strong influence of the difference in the principal tortuosities on the attenuation. For the three pseudo waves the maximal value of the dimensionless attenuation is for a big difference in the principal tortuosities around the double of this of a medium difference and for a small difference a half.

These results indicate that in the low frequency range – in contrast to the high frequency range – the orientation of the principal directions of tortuosity plays a secondary role in measured speeds and attenuation. Thus, most likely it cannot be used for geotechnical applications.

3.3 Shear polarization

Shear waves play a particular role in the analysis of anisotropy. This is due to the fact that in isotropic materials the properties of shear waves are independent of the polarization. All waves with an amplitude perpendicular to the direction of propagation have the same speed and the same attenuation. For this reason they are called *S*-waves without indicating the direction of the amplitude on the plane perpendicular to the propagation direction. This is not the case for anisotropic media and, in particular, for porous media with an anisotropic permeability.

In order to investigate the deviation from the plane perpendicular to the propagation direction of the pseudo transversal wave *S*2 the shear polarization factor is built. It is defined by

$$
\begin{aligned}
&d = \left|\mathrm{Re}\frac{V_1^S}{V_2^S}\right| = \left|\mathrm{Re}\frac{N}{D}\right|,\\
&N = \frac{i\pi_0\omega}{\rho^S}\left(\tau^{(1)^2} - \tau^{(2)^2}\right)\sin\alpha\cos\alpha\left(1 - \frac{-\omega^2 + \frac{\mu^S}{\rho^S}k^2}{r\omega^2}\right),\\
&D = \frac{i\pi_0\omega}{\rho^S}\left(\tau^{(1)^2}\cos^2\alpha + \tau^{(2)^2}\sin^2\alpha\right)\left(1 + \frac{-\omega^2 + \frac{\lambda^S + 2\mu^S}{\rho^S}k^2 + \frac{Q}{\rho^S}k^2}{\frac{Q}{\rho^S}k^2 + r\left(-\omega^2 + \kappa k^2\right)}\right) +\\
&\quad + \frac{Q}{\rho^S}k^2 - r\left(-\omega^2 + \kappa k^2\right)\frac{-\omega^2 + \frac{\lambda^S + 2\mu^S}{\rho^S}k^2 + \frac{Q}{\rho^S}k^2}{\frac{Q}{\rho^S}k^2 + r\left(-\omega^2 + \kappa k^2\right)}, \qquad r = \frac{\rho^F}{\rho^S}.
\end{aligned}
\tag{10}
$$

Details on the derivation of N and D can be found in [1], $k(\omega)$ is the solution of the dispersion relation corresponding to the pseudo shear wave.

In Figure 3 several dependencies of the shear polarization factor, i.e. of the deviation of the direction of the pseudo shear wave from the plane perpendicular to the propagation direction, are shown. From the left column it gets obvious, that d both in the limits of the angle α ($\alpha = 0$ and $\alpha = \pi/2$) and of the frequency ($\omega = 0$, $\omega \to \infty$) is zero. Hence, the coincidence of the propagation direction with a principal direction of tortuosity yields pure transversal waves with an amplitude perpendicular to the propagation direction. Simultaneously, in both limits of the frequency waves do not feel the anisotropy of the tortuosity and become pure transversal waves as well.

In both the left and the middle columns of Figure 3 the dependence of the polarization factor d on the frequency and on the angle α is shown for the above mentioned pairs of principle tortuosities – large difference at the top, medium difference in the middle and small difference at the bottom. While in the left column the original values are presented, in the

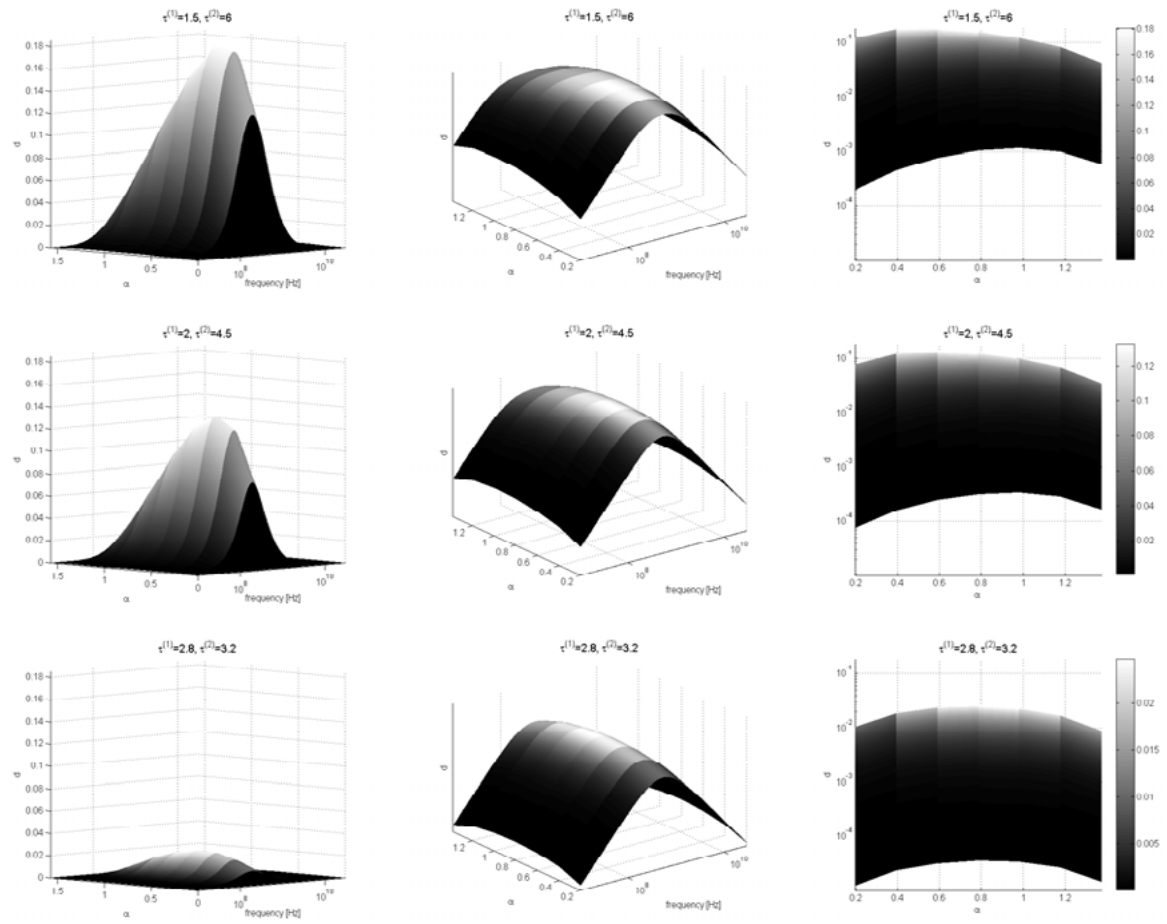

Figure 3: Different views of the shear polarization factor d. Left: as function of frequency and angle α, middle: logarithmic presentation of d, right: range of d in a certain frequency interval in dependence on α. Pairs of tortuosities – top row: $\tau^{(1)} = 1.5$, $\tau^{(2)} = 6.0$, middle row: $\tau^{(1)} = 2.0$, $\tau^{(2)} = 4.5$, bottom row: $\tau^{(1)} = 2.8$, $\tau^{(2)} = 3.2$

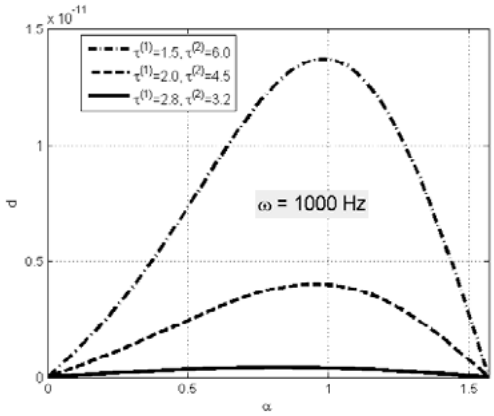

Figure 4: Polarization *d* as a function of angle α in Alermoehe sandstein for three pairs of principal tortuosities

middle column the factor *d* is illustrated logarithmically within the limits $10^{-5} \le d \le 0.185$. On the right-hand side for the range of frequencies $10^7\ \text{Hz} \le \omega \le 3 \cdot 10^{10}\ \text{Hz}$ the polarization factor – also logarithmically – is shown in dependence on α. The maximum of *d* for different angles α varies between around 0.18 for a big difference of the principal tortuosities, 0.13 for a medium difference and 0.02 for a small difference.

Inspection of the left-hand side of the figure immediately points up the limit values of *d*. From middle and right columns – due to the logarithmic presentation – these limits are not evident. However, these figures show that the difference in the tortuosities is not that important for the frequency dependence than for the α-dependence.

Additional to the presentations of *d* for high frequencies, in Figure 4 for a value of the frequency appearing in geotechnics (ω = 1000 Hz) the dependence on α is presented in normal scale. In this way, again, the limits get obvious and the differences for the three choices of principal tortuosities become evident as well even if the values are very small (of the order of 10^{-11}).

The above numerical results show, similarly to the dependencies of speeds and attenuations on the angle α, that a particular orientation of the principal directions of the tortuosity tensor with respect to the propagation direction is of bigger influence for higher frequencies than for lower ones. The anisotropy is primarily reflected by the influence of the principal tortuosities on the attenuation of monochromatic waves and this gives rise to a possibility of a new method of nondestructive acoustic testing of the permeability of geomaterials. For such a method the polarization of the shear waves would be of high importance.

4 CONCLUSIONS

- In a two-component poroelastic material with anisotropic permeability for a special choice of orientation of the propagation direction four waves occur: a transversal mode *S*1, a pseudo transversal mode *S*2 and two pseudo longitudinal waves *P*1 and *P*2.
- In contrast to the high frequency region, in the range of low frequencies – appearing in geotechnical applications – the orientation of principal directions of tortuosity is of

marginal importance for speeds and attenuations.

- Even though, the different permeabilities in different directions may be measured: Due to the appearance of two shear modes a device may be constructed which induces shear waves of different polarization and different propagation directions. A comparison of the amplitudes of arrivals for different polarization of signals would give rise to the principal values and directions of the tortuosity. This would be a nondestructive test of geophysical materials and could be used in applications as seepage processes in road and dam constructions or tunneling in rocks.

REFERENCES

[1] Albers, B., and Wilmanski, K. Acoustics of two-component porous materials with anisotropic tortuosity. *Continuum Mech. Thermodyn.* (2012) **24**(4):403-416.

[2] Albers, B., and Wilmanski, K. Modeling acoustic waves in saturated poroelastic media. *J. Eng. Mech. ASCE* (2005) **131**:974-985.

[3] Arnold, J. *Mobile NMR for rock porosity and permeability*. PhD-thesis, RWTH Aachen, (2007).

[4] Bear, J., and Bachmat, Y. *Introduction to Modeling of Transport Phenomena in Porous Media*. Kluwer, Dordrecht, (1991).

[5] Wang, R., Pavlin, T., Rosen, M.S., Mair, R.W., Cory, D.G., and Walsworth, R.L. Xenon NMR measurements of permeability and tortuosity in reservoir rocks. *Magn. Res. Im*. (2005) **23**(2):329–331.

[6] Wilmanski, K. Monochromatic waves in saturated porous materials with anisotropic permeability. *ZAMM* (2012) **92**(6):452-461.

[7] Wilmanski, K. A few remarks on Biot's model and linear acoustics of poroelastic saturated materials. *Soil Dynamics & Earthquake Engineering* (2006) **26**(6-7):509-536.